Magnetism and superconductivity driven by identical $4f$ states in a heavy-fermion metal

Sunil Nair *, O. Stockert *, U. Witte † ‡, M. Nicklas *, R. Schedler ‡, K. Kiefer ‡, J. D. Thompson §, A. D. Bianchi ¶, Z. Fisk ¶, S. Wirth *, and F. Steglich *

*Max-Planck-Institut für Chemische Physik fester Stoffe, D-01187 Dresden, Germany,†Institut für Festkörperphysik, TU Dresden, D-01062 Dresden, Germany,‡Helmholtz-Zentrum Berlin für Materialien und Energie, D-14109 Berlin, Germany,§Los Alamos National Laboratory, Los Alamos, NM 87545, USA, and ¶University of California, Irvine, CA 92697, USA

Submitted to Proceedings of the National Academy of Sciences of the United States of America

The apparently inimical relationship between magnetism and superconductivity has come under increasing scrutiny in a wide range of material classes, where the free energy landscape conspires to bring them in close proximity to each other. This is particularly the case when these phases microscopically interpenetrate, though the manner in which this can be accomplished remains to be fully comprehended. Here, we present combined measurements of elastic neutron scattering, magnetotransport, and heat capacity on a prototypical heavy fermion system, in which antiferromagnetism and superconductivity are observed. Monitoring the response of these states to the presence of the other, as well as to external thermal and magnetic perturbations, points to the possibility that they emerge from different parts of the Fermi surface. This enables a single $4f$ state to be both localized and itinerant, thus accounting for the coexistence of magnetism and superconductivity.

superconductivity | antiferromagnetism | heavy fermion

The ground state properties of a system are of fundamental importance and the starting point for considering the excitations that enliven real systems. The prevalent electronic ground states of metals, magnetism and superconductivity, are typically mutually exclusive quantum many body phenomena. This antagonism can be evaded by spatial separation (e.g. in some Chevrel phases [1]) or by subdividing the $5f$ states in some actinide compounds into more localized and more itinerant parts giving rise to magnetism or participating in superconductiviy, respectively (see, e.g. [2]). The quest for microscopic coexistence of these phenomena involving *identical* electrons is fueled by the expectation for insight into the complex behavior of new materials with intertwined ground states as, e.g., the cuprate superconductors. Experimentally, this not only requires finding an appropriate material, but also calls for a concerted investigation of both the charge and the spin channel and hence, judiciously chosen measurement methods.

The heavy fermion metals offer an interesting playground where magnetism and superconductivity can both compete and coexist. In these systems, the hybridized f electrons are not only responsible for long-range magnetic order, but are also involved in superconductivity. In this context the CeMIn$_5$ (where M = Co, Ir or Rh) family of heavy fermion metals has been in vogue due to their rich electronic phase diagrams in which an intricate interplay between superconductivity and magnetism is observed [3]. For instance, in CeCoIn$_5$, a superconducting ground state is found below a transition temperature $T_c \approx 2.3$ K whereas CeRhIn$_5$ orders antiferromagnetically below $T_N \approx 3.7$ K [3]. On the other hand, superconductivity is observed in the latter compound by application of pressure whereas the proximity to magnetism in CeCoIn$_5$ is demonstrated by the likely existence of a zero temperature magnetic instability [3]. Moreover, neutron scattering experiments indicate strong antiferromagnetic (AF) quasielastic excitations at wavevectors $Q = (\frac{1}{2}\frac{1}{2}\frac{1}{2})$ and equivalent positions in the paramagnetic regime [4]. However, the excitations become fully inelastic when entering the superconducting state, resulting in the appearance of a spin resonance. These findings underline the analogy to the cuprate high-temperature superconductors [5, 6].

We conducted a comprehensive investigation of the magnetic order and superconductivity in CeCo(In$_{0.9925}$Cd$_{0.0075}$)$_5$. Neutron scattering, magnetotransport and heat capacity, i.e., microscopic and macroscopic, spin and charge sensitive studies have been combined on flux-grown single crystals of the same batch. These combined efforts not only allow to unambiguously pin down the associated effects but also to cross-fertilize the methods. We find a local duality of the electronic $4f$ degrees of freedom implying electronic phase separation on the Fermi surface.

The specific composition with $x = 0.0075$ was chosen since $T_c \approx 1.7$ K and $T_N \approx 2.4$ K are closest within the

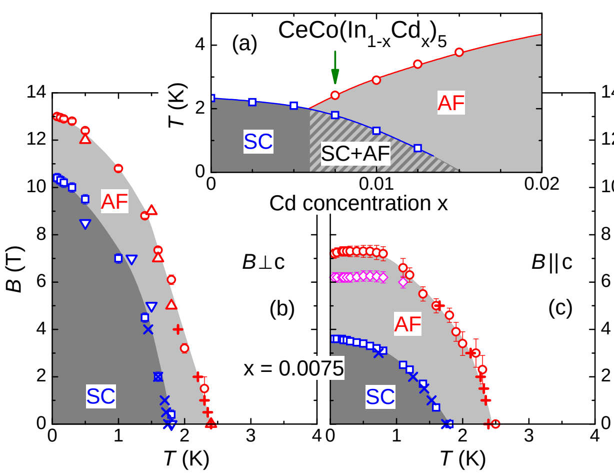

Fig. 1. (a) Doping x dependence of antiferromagnetic (AF) and superconducting (SC) transition temperatures in CeCo(In$_{1-x}$Cd$_x$)$_5$ for Cd-content $x \leq 0.02$ (after Ref. [7]). The crystals investigated here (arrow) exhibit both transitions. (b) B–T phase diagram of CeCo(In$_{0.9925}$Cd$_{0.0075}$)$_5$ obtained from magnetotransport ($\circ, \square$), neutron scattering ($\triangle, \triangledown$) and heat capacity ($+, \times$) measurements with $B \perp c$. (c) B–T diagram for $B \parallel c$ from magnetotransport and heat capacity. Indications of a transition within the AF phase are found ($\diamond$).

Reserved for Publication Footnotes

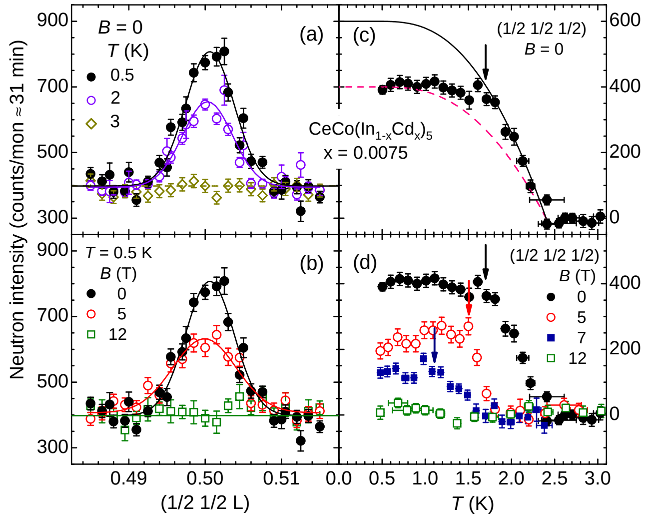

Fig. 2. Elastic neutron scattering scans in $\mathrm{CeCo(In_{0.9925}Cd_{0.0075})_5}$ along $[001]$ and across $(\frac{1}{2}\frac{1}{2}\frac{1}{2})$: (a) at different temperatures in zero magnetic field and (b) for several magnetic fields at $T = 0.5$ K. Solid lines indicate fits with Gaussian lineshape to the data. (c) Temperature dependence of the magnetic intensity at $(\frac{1}{2}\frac{1}{2}\frac{1}{2})$ in $B = 0$ along with fits from mean-field expectations to the data (solid and dashed lines, see text). (d) Same as (c) in addition with data for several magnetic fields. The paramagnetic background contribution was subtracted from data in (c) and (d).

$\mathrm{CeCo(In_{1-x}Cd_x)_5}$ series [7], Fig. 1(a). Consequently, the interplay between superconductivity and antiferromagnetism is expected to be most pronounced [8]. Earlier studies [9, 10] were conducted on samples with $x \geq 0.01$ where T_c is small compared to T_N. Thus, the condensation of conduction electrons into Cooper pairs effectively took place in a state where fluctuations of the AF order parameter were not appreciably large, i.e., where the balance of the two phenomena is already shifted toward AF order. As a result, no significant anomaly in the magnetic intensity as determined by neutron scattering was observed on entering the superconducting regime [10].

The resulting magnetic field–temperature (B–T) phase diagrams are presented in Fig. 1(b) and (c) for $B \perp c$ and $B \parallel c$, respectively. The excellent agreement of results obtained by three very different methods evidences that bulk properties are probed. The strikingly equivalent behavior of the superconducting and AF phase boundary, in particular for $B \perp c$, is indicative of a mutual influence of the two phenomena. The steep initial slope of $T_c(B)$ of approximately $-13(-4)$ T/K for $B \perp (\parallel)\, c$ indicates a large effective quasiparticle mass, i.e., heavy fermion superconductivity.

Initial elastic scans at the lowest temperature ($T = 0.5$ K) across the nuclear peaks confirmed the tetragonal crystal structure, with lattice parameters $a = 4.595$ Å and $c = 7.533$ Å. To search for magnetic intensity, scans along high-symmetry directions were performed. Well below $T_N \approx 2.4$ K and $T_c \approx 1.7$ K, scans along $(\frac{1}{2}\frac{1}{2}l)$ revealed additional magnetic intensity at $(\frac{1}{2}\frac{1}{2}\frac{1}{2})$ and symmetry equivalent positions, see data at $T = 0.5$ K in Fig. 2(a). Above T_N this magnetic superstructure peak completely vanished, *cf.* Fig. 2(a) for data at $T = 3$ K. The scans did not indicate additional intensity at other, e.g. incommensurate, positions. In particular, no magnetic superstructure peaks were detected around $(\frac{1}{2}\frac{1}{2}0.3)$ or $(\frac{1}{2}\frac{1}{2}0.4)$, which have been observed in the closely related system $\mathrm{CeRhIn_5}$ [11]. The commensurate magnetic structure is therefore in close agreement with that reported earlier on the 1% Cd doped sample [10]. Elastic scans across $(\frac{1}{2}\frac{1}{2}\frac{1}{2})$ at $T = 0.5$ K and for several magnetic fields are displayed in Fig. 2(b). Obviously, a magnetic field of $B = 12$ T suffices to fully suppress antiferromagnetism at this temperature. More importantly, the observation of a magnetic superstructure peak in zero magnetic field well inside the superconducting state clearly demonstrates the coexistence of AF order and superconductivity on a microscopic scale. Based on our heat capacity measurements we emphasize that both, the transition into the AF ordered and the superconducting state, are bulk transitions.

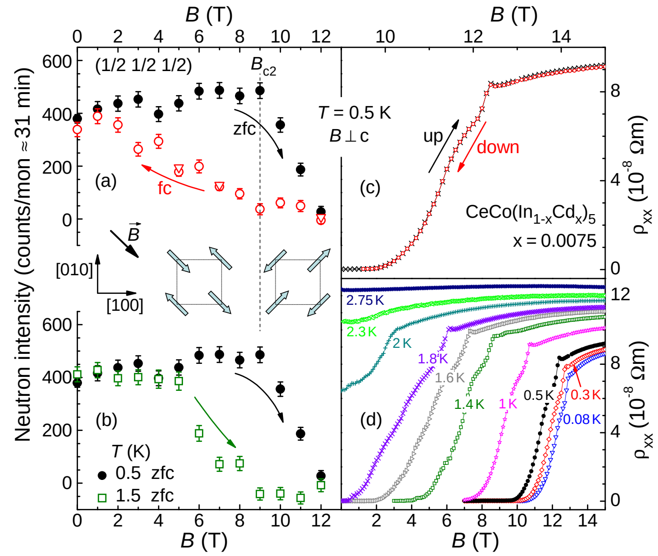

Fig. 3. Comparison of neutron scattering and resistivity measurements. (a) Field dependent magnetic intensity at $(\frac{1}{2}\frac{1}{2}\frac{1}{2})$ and $T = 0.5$ K after zero-field cooling (zfc) and field cooling (fc, ▽). Arrows indicate the direction of magnetic field variation. The different field conditions give rise to different domain population as shown in the inset: For fc and $B > B_{c2}$ (B_{c2} is marked by the dashed line) only the depicted spin configuration in the basal plane is found, below B_{c2} also the second displayed domain (left) is increasingly occupied. (b) Magnetic intensity after zfc at $T = 0.5$ K and 1.5 K. (c) Field dependence of resistivity ρ_{xx} for $B \perp c$. A protocol analogous to (a) has been followed, yet no significant hysteresis was found. (d) Resistivity ρ_{xx} as function of B ($\perp c$) displayed for selected temperatures.

In order to scrutinize the possible influence of superconductivity on the AF order, the magnetic intensity at $(\frac{1}{2}\frac{1}{2}\frac{1}{2})$ was recorded as a function of temperature for different magnetic fields, Figs. 2(c) and (d). In zero magnetic field the magnetic intensity increases below T_N and displays a kink at T_c (marked by arrows) with no further change in intensity at lower temperatures. For increasing magnetic field, T_N and the overall magnetic intensity are reduced. No magnetic intensity was detected for $B = 12$ T. The assignment of this kink to T_c is corroborated by the magnetotransport and heat capacity measurements. An attempt to fit the zero-field magnetic intensity by a mean-field model for the sublattice magnetization (using a Brillouin function for an effective spin-$\frac{1}{2}$ system) fails to describe the whole temperature dependence, as indicated by the dashed line in Fig. 2(c). On the other hand, a fit restricted to the temperature range $T_c < T < T_N$ reproduces these data reasonably well [solid line in Fig. 2(c)] and results in an expected magnetic intensity for $T \to 0$ of about 40% larger than the experimentally observed saturation value. Obviously, the onset of superconductivity *prevents a further rise* of magnetic intensity below T_c *without suppressing* the AF order itself.

The magnetic intensities measured as a function of applied field $B \parallel [1\bar{1}0]$ for different temperatures and different protocols are directly compared to magnetotransport $\rho_{xx}(B)$ in Fig. 3 facilitating again a clear assignment of the observed

features. The disappearance of magnetic intensity, signaling the transition from the antiferromagnetically ordered phase to a paramagnetic one, nicely concurs with the strong change in slope in $\rho_{xx}(B)$. On the other hand, the kink in the field-dependent neutron intensity can be identified as the superconducting upper critical field B_{c2} coinciding with the approach to zero resistivity. The latter is also supported by the similarity of the field-dependent neutron intensity [Fig. 3(b)] and its temperature dependence, Fig. 2(d).

Interestingly, a pronounced hysteresis is seen for the neutron scattering intensities taken at increasing (zfc) and decreasing magnetic field, Fig. 3(a). Whereas the aforementioned kink is observed for increasing magnetic field, in decreasing field the magnetic intensity grows steadily and only reaches for $B \to 0$ the values of the zero-field cooled measurements. In the pristine $CeCoIn_5$, a multi-component ground state (also discussed as a possible Fulde-Ferrel-Larkin-Ovchinnikov phase) with characteristics of a first order phase transition has been observed at low temperatures ($T < 0.3$ K) in fields $B > 10$ T applied along the $[1\bar{1}0]$ direction [12, 13]. However, in accord with the sensitivity of such a state to disorder its existence in the Cd substituted system has been dismissed [14]. It is to be noted that enhanced disorder arising from Cd substitution increases the typical resistivity values in this system by an order of magnitude in comparison to undoped $CeCoIn_5$. Moreover, the range of magnetic fields within which this hysteresis is observed in neutron scattering implies that the hysteretic behavior is seen mainly above B_{c2} within the AF phase, ruling out shielding effects. An alternative scenario would involve that the field-driven transition from an AF phase into a paramagnetic one is first order in nature. To investigate this possibility, we have performed resistivity measurements in slowly increasing and decreasing fields at $T = 0.5$ K. As shown in Fig. 3(c), no significant hysteresis is observed indicating that the field-driven transition is continuous in character (at least for $T \geq 0.06$ K).

With the first order scenario likely ruled out, the observed hysteresis in our neutron scattering data (and the lack of it in ρ_{xx}) can only be explained by invoking the possibility of two different domain populations in the field cooled and zero field cooled measurements. Though relatively little explored in comparison to ferromagnets, the existence of magnetic domains is well established for anisotropic antiferromagnets. A particularly well investigated example is elemental Cr for which the influence of different domain populations as a function of measuring protocols has been observed [15, 16]. Our neutron data indicate an unequal domain population upon entering the magnetically ordered state at low temperatures and high magnetic fields. Decreasing the magnetic field at low T and crossing the phase boundary into the AF state, one domain configuration [with magnetic moments $\perp B$, *cf.* Fig. 3(a)] is strongly favored over the other (with magnetic moments $\parallel B$) resulting in a substantially reduced magnetic intensity in neutron scattering measurements (see *Materials and Methods* section). Further reducing the magnetic field and inside the superconducting state the second domain successively becomes populated balancing the domain population when reaching $B = 0$, identical to the zfc case. The associated domain walls strongly influence the magnetotransport *only* if the electronic mean free path ℓ is comparable to or larger than the domain wall thickness δ [15]. The lack of hysteresis in our transport measurements suggests that this criterion is not met in the $B \perp c$ direction, i.e., $\delta \gg \ell$. Note that even in undoped $CeCoIn_5$, ℓ is reduced to a few ten nm already in moderate fields [17]. However, we were able to resolve a tiny hysteresis ($\lesssim 0.2$ T at 0.2 K) in the magnetoresistance for $B \parallel c$

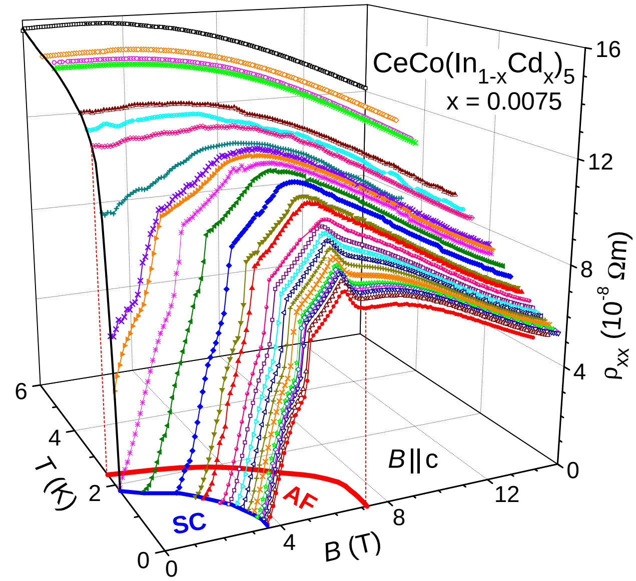

Fig. 4. (a) Magnetic field dependence of the resistivity ρ_{xx} as measured in $CeCo(In_{0.9925}Cd_{0.0075})_5$ at different temperatures with $B \parallel c$. The phase boundaries associated with superconductivity and antiferromagnetism are marked.

within the AF regime [18]. This observation is consistent with an enhanced (factor of 1.5) dynamic spin correlation length within the ab plane compared to the c direction [4, 19] which indicates a reduced δ in c direction.

In order to trace the anisotropic nature of the superconductivity and magnetism in this system, we also measured ρ_{xx} with field applied along the crystallographic c axis. This is shown in Fig. 4, with the zero-resistance superconducting state and the field-induced destabilization of AF order being clearly marked out. At lowest temperature and for decreasing field, the sharp increase in resistivity at $B \sim 7$ T indicates carrier localization due to the onset of AF order. On further reduction of the magnetic field, a drop in $\rho_{xx}(B)$ for $B \lesssim 6$ T is observed within the AF state. This could possibly originate from a spin rearrangement as found in $CeCu_5Au$ [20], a scenario that would also account for the observed anisotropy in $\rho_{xx}(B)$. Alternatively, one might speculate that the drop in $\rho_{xx}(B)$ may be caused by a change in ordering vector as, e.g., observed $CeCu_2Si_2$ [21]. The signatures of these two transitions merge as they become broadened at increasing temperatures. The magnetoresistance is negative down to $T = 0.06$ K for 7 T $\lesssim B \leq 15$ T manifesting that there is *no* Fermi liquid regime in the investigated field range. This effectively rules out the presence of a quantum critical point in the $B \parallel c$ direction. Interestingly, for $B \perp c$ the destruction of long-range AF order is succeeded by a field range of positive magnetoresistance which indicates that the system enters into a regime with coherent Kondo scattering [22]. Analyzing $\rho_{xx}(T)$ for constant fields did not reveal any signature of a T^2 dependence eliminating the possibility of Fermi liquid behavior also for $B \perp c$ [a Kohler's scaling analysis is hampered by large uncertainties in $\rho_{xx}(0)$].

The almost constant neutron intensity below T_c is intriguing. Its analysis above and the electronic transport measurements indicate a second order phase transition at T_c without spatial phase separation. Then, the deviation of the neutron intensity from its expected value below T_c implies coexistence and, more importantly, mutual influence of AF and superconducting order. These conclusions go well beyond those drawn from earlier Nuclear Magnetic Resonance measurements [9]:

Although the microscopic coexistence of AF and superconducting order was inferred, the interplay between the two different types of order was not observed. Based on our new measurements we speculate that the low-energy magnetic fluctuations are gapped by superconductivity and likely shifted to higher energies (possibly to the resonance at 0.6 meV observed in undoped $\mathrm{CeCoIn_5}$ [4]), a similar mechanism as discussed for the cuprates [23]. The delicate, unprecedented balance of the two states may result from the proximity of T_c and T_N in the chosen compound. Since the commensurability of the AF order with $\tau = (\frac{1}{2}\frac{1}{2}\frac{1}{2})$ and NMR studies [9] suggest mainly local magnetism, the single $4f$ state spans both local and itinerant character in momentum space. We note that the local coexistence of AF and superconducting order is corroborated by the spin-spin correlation length ξ_m clearly exceeding the superconducting one, ξ_{GL}. The former can be estimated from the broadened (beyond resolution) Gaussians of the neutron scattering intensities (*cf.*, e.g., Fig. 2(a)), $\xi_m \approx 32$ nm, whereas an upper bound $\xi_{GL} \lesssim 10$ nm can be inferred from the estimated critical field $B_{c2}(T \to 0)$.

In conclusion, magnetotransport, heat capacity and elastic neutron scattering measurements were combined to unambiguously identify the respective features of antiferromagnetic and superconducting order in the heavy-fermion alloy $\mathrm{CeCo(In_{1-x}Cd_x)_5}$ with $x = 0.0075$ resulting in a highly consistent B–T phase diagram. Below T_c, superconductivity and magnetism correlate via identical $4f$ states resulting in a delicate balance of local coexistence. The phase transitions appear to be continuous in nature, and the pronounced hysteresis observed in neutron scattering measurements likely arises from different domain populations dictated by the sample history. The destruction of antiferromagnetic order at lowest temperature is *not* followed by Fermi liquid behavior for a substantial field range leaving the ground state unresolved.

Materials and Methods

A 12 mg platelet-like single crystal was used for neutron scattering as well as for heat capacity measurements in a commercial Physical Property Measurement System with ^{3}He insert. Magnetoresistance measurements were conducted with $B \leq 15$ T applied both $\parallel c$ and $\perp c$ for 0.06 K $\leq T \leq$ 6 K.

Elastic neutron scattering measurements were conducted in the temperature range 0.5 K $\leq T \leq 3$ K within the $[110]-[001]$ horizontal scattering plane, both in field cooled (fc) and zero-field cooled (zfc) conditions. Magnetic fields $B \leq$ 12 T were applied within the basal **ab** plane. These measurements were performed on the thermal triple-axis spectrometer E1 at the BER-II reactor of the Helmholtz-Zentrum Berlin für Materialien und Energie in Berlin/Germany.

With respect to our discussion of magnetic domains it should be noted that the neutrons can only couple to moments perpendicular to the momentum transfer **Q**. In our case, this allows to unambiguously assign a largely reduced magnetic intensity at $\mathbf{Q} = (\frac{1}{2}\frac{1}{2}\frac{1}{2})$ and high magnetic fields B to such domains with magnetic moments perpendicular to B since only for these domains there are components of the magnetic moment parallel to **Q**. In contrast, for the domains with magnetic moments parallel to B all individual moments are aligned perpendicular to **Q** which results in a much higher neutron intensity.

ACKNOWLEDGMENTS. This work was partially supported by the DFG Research Unit 960 "Quantum Phase Transitions". Z.F. acknowledges support through NSF-DMR-071042. Work at Los Alamos National Laboratory was performed under the auspices of the U.S. Department of Energy, Office of Science.

1. Fischer Ø (1978) Chevrel phases - superconducting and normal state properties. Appl. Phys. 16:1-28.
2. Sato NK, et al. (2001) Strong coupling between local moments and superconducting 'heavy' electrons in $\mathrm{UPd_2Al_3}$. Nature 410:340-343.
3. Sarrao JL and Thompson JD (2007) Superconductivity in cerium- and plutonium-based '115' materials. J. Phys. Soc. Jpn. 76:051013.
4. Stock C, Broholm C, Hudis J, Kang HJ, Petrovic C (2008) Spin resonance in the d-wave superconductor $\mathrm{CeCoIn_5}$. Phys. Rev. Lett. 100:087001.
5. Sidis Y, et al. (2004) Magnetic resonant excitations in high-T_c superconductors. phys. stat. sol. (b) 241:1204-1210.
6. Hayden SM, Mook HA, Dai PC, Perring TG, Dogan F (2004) The structure of the high-energy spin excitations in a high-transition-temperature superconductor. Nature 429:531-534.
7. Pham LD, Park T, Maquilon S, Thompson JD, Fisk Z (2006) Reversible tuning of the heavy-fermion ground state in $\mathrm{CeCoIn_5}$. Phys. Rev. Lett. 97:056404.
8. Kato M and Machida K (1988) Superconductivity and spin-density waves - Application to Heavy-fermion materials. Phys. Rev. B 37:1510-1519.
9. Urbano RR, et al. (2007) Interacting Antiferromagnetic Droplets in Quantum Critical $\mathrm{CeCoIn_5}$. Phys. Rev. Lett. 99:146402.
10. Nicklas M, et al. (2007) Magnetic structure of Cd-doped $\mathrm{CeCoIn_5}$. Phys. Rev. B 76:052401.
11. Bao W, et al. (2000) Incommensurate magnetic structure of $\mathrm{CeRhIn_5}$. Phys. Rev B 62:R14621-R14624.
12. Bianchi A, Movshovich R, Capan C, Pagliuso PG, Sarrao JL (2003) Possible Fulde-Ferrell-Larkin-Ovchinnikov superconducting state in $\mathrm{CeCoIn_5}$. Phys. Rev. Lett. 91:187004.
13. Kenzelmann M, et al. (2008) Coupled superconducting and magnetic order in $\mathrm{CeCoIn_5}$. Science 321:1652-1654.
14. Tokiwa Y, et al. (2008) Anisotropic effect of Cd and Hg doping on the Pauli limited superconductor $\mathrm{CeCoIn_5}$. Phys. Rev. Lett. 101:037001.
15. Jaramillo R, et al. (2007) Microscopic and macroscopic signatures of antiferromagnetic domain walls. Phys. Rev. Lett. 98:117206.
16. Kummamuru RK, Soh Y-Ah (2008) Electrical effects of spin density wave quantization and magnetic domain walls in chromium. Nature 452:859-863.
17. Kasahara Y, et al. (2005) Anomalous quasiparticle transport in the superconducting state of $\mathrm{CeCoIn_5}$. Phys. Rev. B 72:214515.
18. Nair S, et al. (2009) Hall effect and magnetoresistance in the heavy fermion superconductor $\mathrm{CeCo(In_{1-x}Cd_x)_5}$. J. Phys.: Conf. Series 150:042133.
19. Curro NJ and Pines D (2007) Anisotropic spin fluctuations in $\mathrm{CeCoIn_5}$ J. Phys. Chem. Solid 68:2028-2030.
20. Paschke C, Speck C, Portisch G, von Löhneysen H (1994) Magnetic-ordering and Kondo compensation in the ternary heavy-fermion compound $\mathrm{CeCu_5Au}$. J. Low Temp. Phys. 97:229-250.
21. Gegenwart P, et al. (1998) Breakup of heavy fermions on the brink of 'phase A' in $\mathrm{CeCu_2Si_2}$. Phys. Rev. Lett. 81:1501-1504.
22. Brandt NB and Moshchalkov VV (1984) Concentrated Kondo systems. Adv. Phys. 33:373-467.
23. Dahm T, et al. (2009) Strength of the spin-fluctuation-mediated pairing interaction in a high-temperature superconductor. Nature Phys. 5:217-221.